Platinum-group minerals in the Selukwe Subchamber, Great Dyke, Zimbabwe: implications for PGE collection mechanisms and post-formational redistribution

BRONWEN M. COGHILL AND ALLAN H. WILSON

Department of Geology, University of Natal, P.O. Box 375, Pietermaritzburg 3200, South Africa

Abstract

This paper presents the results of microprobe investigations of the Platinum-Group Elements (PGE) of the Selukwe Subchamber, Great Dyke, Zimbabwe. The PGE are associated with base metal sulphides in the uppermost pyroxenites of the Ultramafic Sequence of the Great Dyke. The following minerals have been indentified: bismuthotellurides (moncheite, maslovite, michenerite, kotulskite and polarite); arsenides (sperrylite); and sulphides and sulpharsenides (cooperite, laurite, braggite and hollingworthite). Platinum Group Minerals (PGM) occur in three distinct textural environments: (1) at the boundary of sulphides and silicates/hydrosilicates, (2) entirely enclosed within sulphides, and (3) entirely enclosed within silicate or hydrosilicate minerals. The stratigraphic distribution, environments and textures of the PGM have important genetic implications, and cannot be explained by a single process. A multi-process model for the petrogenesis of the PGE mineralisation in terms of complexation and intermediate compound formation is proposed. The primary mineralising events were due to orthomagmatic processes, but the observed textures are the result of microscale remobilisation of PGM components by trapped interstitial fluids (hydromagmatic processes).

KEYWORDS: Platinum Group Elements, Zimbabwe, Great Dyke, microprobe investigations, Affinity Factor.

Introduction

THE presence of platinum associated with sulphide deposits in the Great Dyke was first reported over 70 years ago (Zealley, 1918) and in several subsequent reports (Lightfoot, 1926, 1927; Wagner, 1929). Only in recent years has the geology of the platinum ore zone of the Great Dyke been described in detail and evaluated on an economic basis. The complexity of the ore zone, combined with low market prices in the 1970s, resulted in the failure of successful economic development of this resource, despite extensive drilling investigations and numerous trial mining operations carried out by several exploration companies. In recent years there has been renewed economic interest in this commodity resulting in a number of detailed studies of the Main Sulphide Zone and the PGE mineralisation, e.g. Wilson *et al.*, 1989; Prendergast and Keays, 1989; Wilson and Tredoux, 1990; Prendergast, 1990; and Evans and Buchanan, 1991.

The platinum-group mineralogy has been documented for the Darwendale Subchamber by Johan *et al.* (1989) and, in a recent detailed study of the Wedza–Mimosa deposit in the southern part of the Great Dyke, Prendergast (1990) illustrates the importance of understanding the mineral associations and their implications for PGE recovery. The present study is the first reported account on the Selukwe Subchamber. Previous studies on the Great Dyke platinum deposit have identified the main PGE-bearing phases as being sperrylite, cooperite, braggite and Pt- and Pd-bearing bismuthotellurides (Wagner, 1929; Schweigart, 1967; Schweigart and Fasso, 1967; Haynes, 1983; Evans and Buchanan, 1991), and attention is drawn to the mutual occurrence of both high- and low-temperature mineral assemblages.

Central to the understanding of the PGE deposits is whether these originated by wholly magmatic processes (Campbell and Barnes, 1984)

Mineralogical Magazine, December 1993, Vol. 57, pp. 613–633

or whether transport of the metals occurred by hydrothermal fluids (e.g. Boudreau *et al.*, 1986). Evaluation of these two contrasting processes may be made only on the basis of detailed mineralogical studies. The results of this study show that no single process can account for the observed mineralisation pattern, and a complex multi-stage mechanism is proposed.

Geological setting

The Great Dyke. The Great Dyke of Zimbabwe is an early Proterozoic layered intrusion of mafic and ultramafic rocks, some 550 km long, set in an Archaean granite–greenstone terrain of the Zimbabwe Craton (Wilson and Prendergast, 1989) (Fig. 1). It is trumpet-shaped in cross-section, with a postulated dyke-like feeder at depth (Podmore and Wilson, 1987). The shallow dip of the layered sequence towards the central longitudinal axis gives the sequence a synclinal structure (Wilson and Prendergast, 1989).

The Dyke was intruded in two major magma chambers, each comprising smaller subchambers (Fig. 1). The study area is in the Selukwe Subchamber, which represents the northern part of the South Chamber (Wilson and Tredoux, 1990) (Fig. 1). The Selukwe Subchamber, like the other subchambers, comprises a lower Ultramafic Sequence and an upper Mafic Sequence (Fig. 2*a*). The Mafic Sequence is preserved only as gabbroic remnants in the central portions of the Subchamber. The Ultramafic Sequence, comprising mainly chromitites, dunites, harzburgites, olivine bronzitites and bronzitites, is characterised by well-developed cyclic units (Fig. 2*a*).

The P1 Pyroxenite. The uppermost cyclic unit of the Ultramafic Sequence, Cyclic Unit 1 (CU1), occurs immediately below the mafic/ultramafic contact. It is characterised by a pyroxenite layer (the P1 layer), comprising a thick bronzitite layer (approximately 120m thick in the Selukwe Subchamber) and an overlying websterite layer, 3–4m thick at the margin and increasing to a thickness of 9–10 m in the axis (Fig. 2*b*).

The generally medium-grained bronzitite layer comprises cumulus bronzite enclosed by postcumulus augite and plagioclase. The websterite is a bronzite–augite cumulate with postcumulus plagioclase. Interstitial mineral phases include quartz, potassium feldspar, biotite/phlogopite, hornblende, opaques (sulphides, magnetite, and rare chromite, rutile and ilmenite) and accessory titanite, apatite and zircon.

The 'potato reef' is the name given to websterite and bronzitite that has a nodular appearance in weathered outcrop. The 'potatoes' or nodules develop as a result of optically-continuous, zoned plagioclase oikocrysts enclosing fresh bronzite crystals and very little sulphide. The sulphides and late-stage mineral assemblage are concentrated around the oikocryst margins, which, as a result, weather easily to form the subspherical structures of the outcrop. This characteristic nodular pyroxenite was used as a hanging-wall marker for the platinum-bearing sulphide zone by early prospectors in the Darwendale Subchamber (Wilson, 1992).

The P1 layer is significant in the genesis of the Great Dyke because: (1) these pyroxenites occur at the critical transition where augite and plagioclase become the dominant cumulus phases (in the Mafic Sequence), in place of olivine and bronzite (in the Ultramafic Sequence), and (2) it hosts the PGE-enriched sulphide-bearing zones (Wilson and Prendergast, 1989; Prendergast and Keays, 1989; Wilson and Tredoux, 1990; Prendergast, 1990). The P1 pyroxenite is the most complex cyclic unit of the layered intrusion, showing both lateral and vertical changes in textures, lithologies and mineral compositions.

Platinum-group element mineralisation

Sulphide mineralisation and PGE distributions. The Main Sulphide Zone (MSZ) is a thin, persistent, stratiform zone of very high sulphide enrichment (up to 7% sulphide) in the upper P1 layer, and occurs in all subchambers of the Great Dyke. In the study area, it ranges from 2 to 5 m thick (Fig. 2*b*) and overlaps the bronzitite/websterite contact. A broader zone of disseminated sulphide, with a lower sulphide content than the MSZ (up to 1%), occurs lower in the bronzitite layer of P1, and is referred to as the Lower Sulphide Zone (LSZ) (Prendergast and Wilson, 1989). This comprises a complex series of subzones of sulphide mineralisation.

The base metal sulphides (BMS) include pyrrhotite, pentlandite (mainly as exsolution in pyrrhotite), chalcopyrite and pyrite. The BMS occur in a variety of forms. Primary magmatic sulphides occur either as early-formed high-temperature inclusions in cumulus bronzite crystals, or as interstitial phases to the cumulus phases. Where intercumulus sulphides are abundant, they have a subpoikilitic, net-textured appearance; where sparse, they occur as tiny anhedral grains with other interstitial phases. In zones of abundant sulphide, there is a marked increase in alteration of the silicate mineral assemblage. Post-solidus replacement of bronzite, and less commonly augite and plagioclase, has resulted in a hydrosilicate alteration assemblage consisting of tremo-

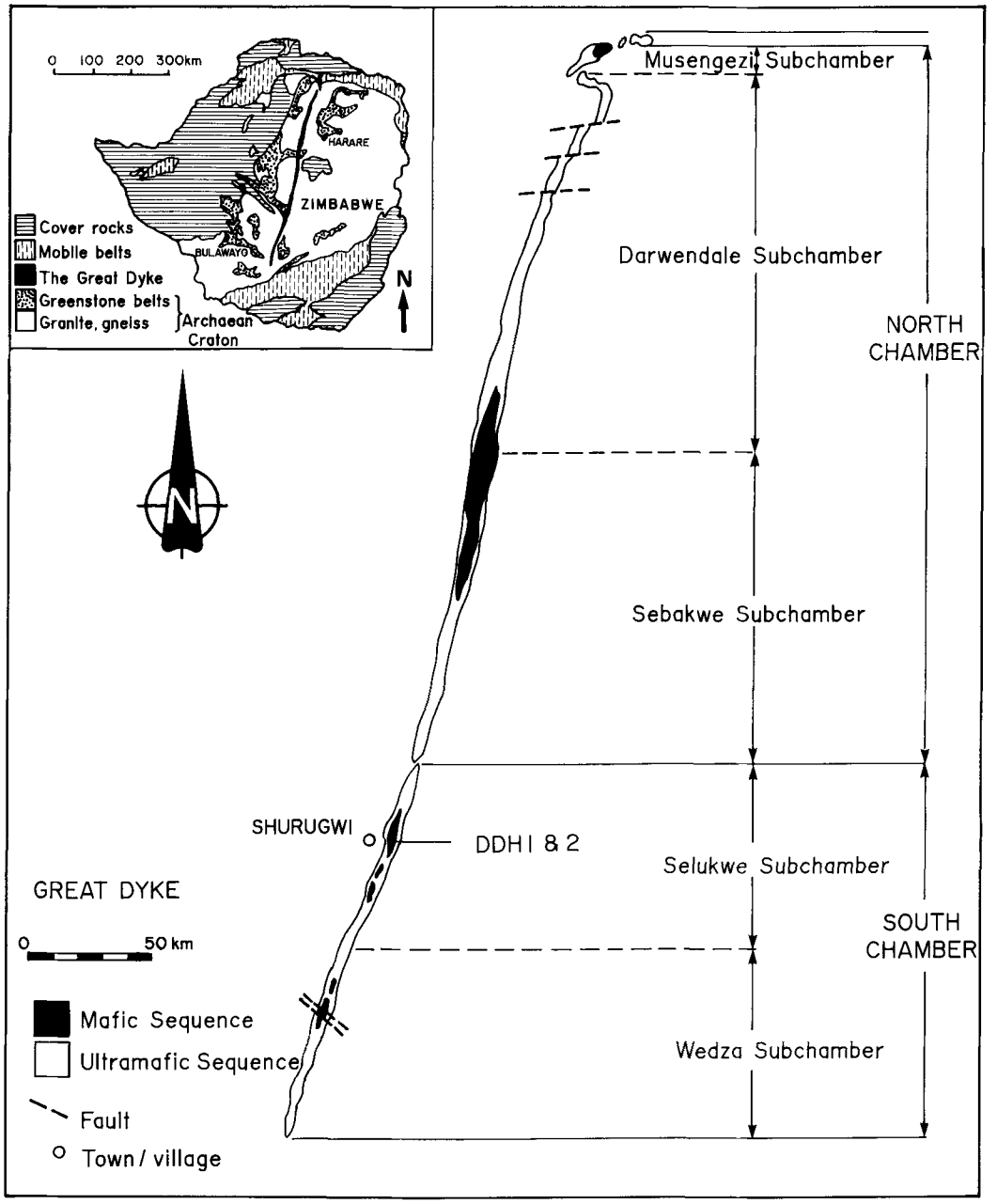

FIG. 1. Map showing the location of the magma chambers and subchambers of the Great Dyke of Zimbabwe, and location of the study area (after Prendergast and Wilson, 1989).

lite, talc, magnetite, biotite, and minor chlorite and epidote (Prendergast, 1990). These hydrosilicates are commonly intergrown with BMS. This assemblage of secondary alteration minerals is texturally distinguishable from primary late-stage hydrous minerals (phlogopite, amphibole and talc) which formed as a consequence of the final stage crystallisation of local pockets of intercumulus liquid. The interaction of pockets of late-stage hydrous magma with the BMS released highly

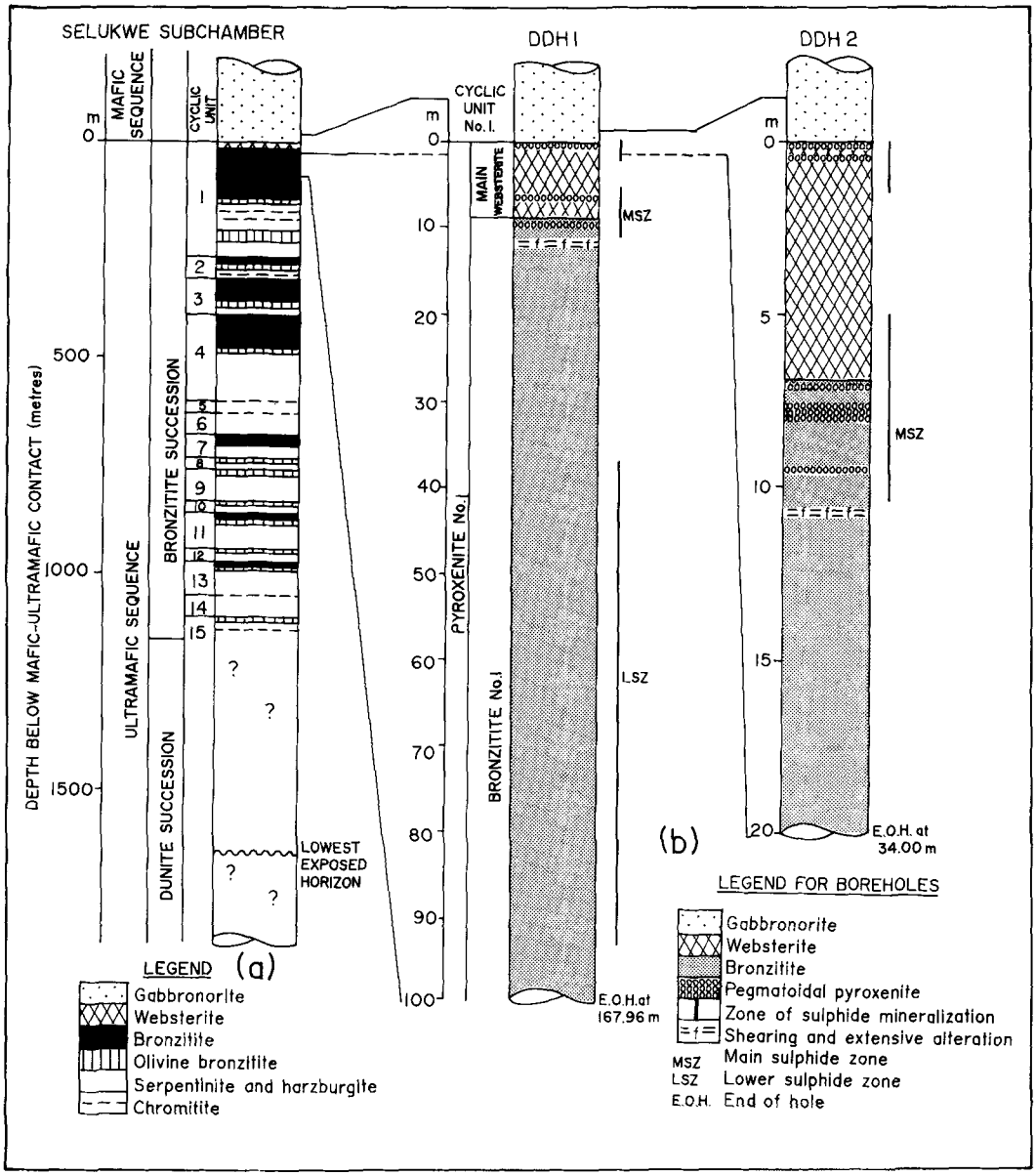

FIG. 2. (*a*) Stratigraphy of the Selukwe Subchamber (after Wilson and Prendergast, 1989). (*b*) Borehole logs for DDH 1 and DDH 2, showing upper pyroxenites of CU1, and positions of the MSZ and LSZ.

corrosive fluids which induced pervasive alteration of early-formed silicates to give the hydrosilicate assemblage.

The vertical distributions of PGE in the sulphide zones in the Selukwe Subchamber (Fig. 3) are broadly similar to those described in the Wedza Subchamber (Prendergast and Keays, 1989; Prendergast, 1990) and Darwendale Subchamber (Wilson *et al.*, 1989; Wilson and Tredoux, 1990). The PGE are characteristically enriched at the base of each of the sulphide zones. In the Main Sulphide Zone (MSZ), PGE values increase gently upwards through the stratigraphy, and then fall sharply above the point of maximum enrichment. In the Lower Sulphide Zone (LSZ), the patterns characteristically show less marked enrichment, with the fall in values following the maximum enrichment occurring as a series of

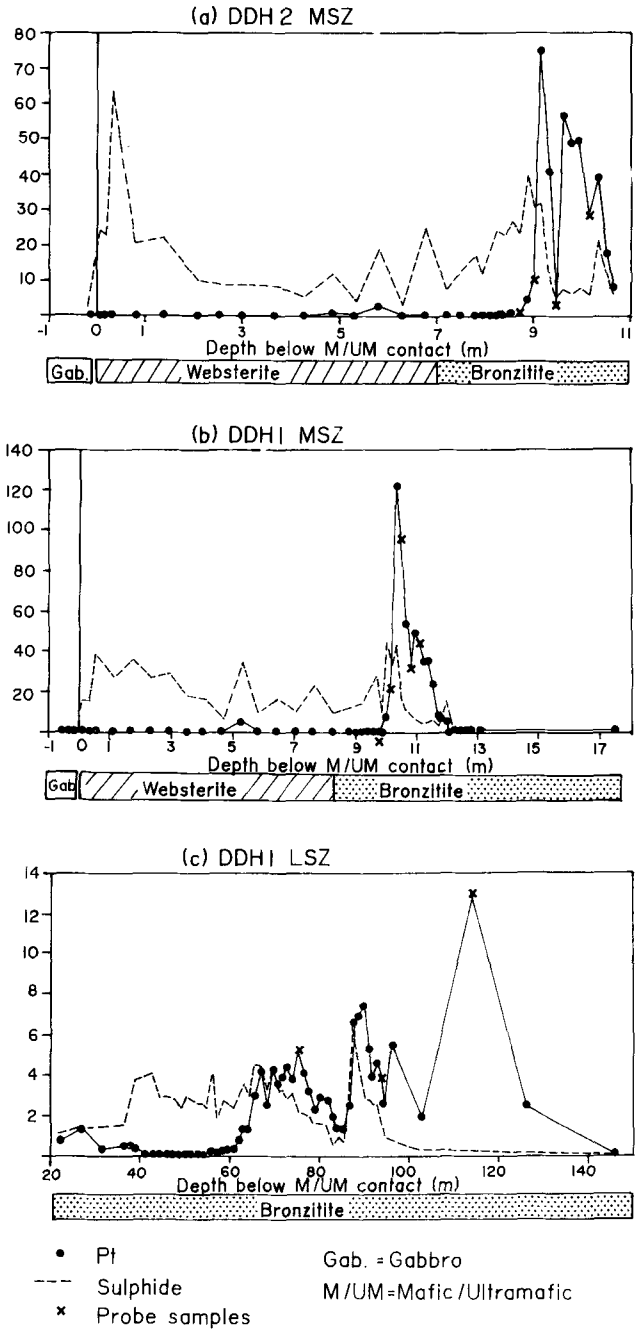

FIG. 3. Stratigraphic distribution of Pt and sulphide in whole rock for (*a*) MSZ of DDH2, (*b*) MSZ of DDH1, and (*c*) LSZ of DDH1. Location of probe samples used in this study is shown. Depth is given relative to the position of the gabbro–websterite boundary. Note that values assigned to the vertical axes are merely illustrative of the relative concentrations of Pt and sulphide in the different boreholes and sulphide zones. Absolute values have been omitted because of confidentiality requirements.

subsidiary peaks, which are progressively less well-developed higher in the stratigraphy. The peak enrichments of PGE in the LSZ all have much lower values than those in the MSZ (Fig. 3).

Sample selection and analytical techniques for determinative PGM mineralogy

Platinum-group minerals (PGM) in the Great Dyke rocks are difficult to locate, because of their generally small size and localised concentration in the vertical profile. The characteristic profiles of the PGE distributions were thus used to aid the selection of suitable borehole core samples for polished thin sections. Twelve samples through the ore zone were chosen from the borehole sections—4 from DDH 2 (MSZ), and 8 from DDH 1 (5 from the MSZ and 3 from the LSZ). The sample positions are indicated on Fig. 3(*a–c*).

The PGM were located and initially qualitatively analysed by means of a scanning electron microscope (SEM). Quantitative analyses using an electron microprobe were for the elements As, Te, Bi, Sb, S, Pt, Pd, Rh, Zn, Cu, Ni and Fe. Analytical details are shown in Table 1.

Inter-element interferences of Pt with Rh and Sb with As had to be considered, with every 1% of Pt, and 1% of Sb contributing approximately

TABLE 1: Representative microprobe analyses for PGM (given in %) and analytical details.

Mineral name	No. an.	As	Te	Fe	Ni	Bi	Pd	Pt	Zn	Sb	S	Cu	Rh	Total
Moncheite		n.d.	33.47	0.84	0.07	27.13	n.d.	33.27	n.d.	0.29	n.d.	0.06	n.d.	100.14
Range (l)	11	n.d.	27.22	0.37	0.05	19.3	n.d.	21.64	n.d.	0.23	n.d.	n.d.	n.d.	
(u)		n.d.	46.60	2.63	2.51	34.77	8.00	36.84	n.d.	0.63	1.30	1.67	0.30	
Sperrylite		44.26	n.d.	0.90	n.d.	n.d.	n.d.	53.73	n.d.	n.d.	0.56	0.11	0.24	100.01
Range (l)	11	41.26	n.d.	0.12	n.d.	n.d.	n.d.	49.96	n.d.	n.d.	0.37	n.d.	0.01	
(u)		44.60	0.15	2.54	1.91	0.13	0.48	55.58	n.d.	0.35	2.94	0.23	2.28	
Cooperite		n.d.	n.d.	2.64	0.51	n.d.	1.72	79.22	n.d.	0.03	15.81	n.d.	0.08	100.08
Range (l)	5	n.d.	n.d.	0.77	0.36	n.d.	0.77	76.12	n.d.	n.d.	15.43	n.d.	n.d.	
(u)		n.d.	n.d.	2.64	0.76	0.12	3.41	81.72	n.d.	0.03	15.81	0.70	0.08	
Braggite		1.41	n.d.	0.85	5.31	n.d.	24.63	48.29	n.d.	n.d.	19.64	0.13	n.d.	100.26
Range (l)	3	n.d.	n.d.	0.85	0.47	n.d.	10.01	48.29	n.d.	n.d.	17.55	n.d.	n.d.	
(u)		1.41	n.d.	4.14	6.77	n.d.	24.63	72.10	n.d.	n.d.	20.50	0.30	0.07	
Maslovite		n.d.	23.12	0.71	0.13	39.60	n.d.	35.03	n.d.	0.22	n.d.	n.d.	n.d.	98.81
Range (l)	3	n.d.	22.77	0.71	n.d.	36.94	n.d.	33.24	n.d.	0.19	n.d.	n.d.	n.d.	
(u)		n.d.	26.23	3.04	0.13	39.60	n.d.	35.03	n.d.	0.24	n.d.	n.d.	n.d.	
Michenerite		n.d.	29.49	1.29	0.13	45.28	24.78	n.d.	n.d.	0.27	0.05	0.48	n.d.	101.81
Range (l)	3	n.d.	28.12	1.02	0.08	43.91	20.27	n.d.	n.d.	0.14	0.50	n.d.	n.d.	
(u)		n.d.	29.49	4.36	1.09	45.28	24.78	3.17	n.d.	0.39	1.57	0.48	n.d.	
Kotulskite		n.d.	26.47	0.66	0.10	32.40	41.22	n.d.	n.d.	0.67	n.d.	0.06	n.d.	102.14
Range (l)	2	n.d.	21.64	0.66	0.07	32.40	40.12	n.d.	n.d.	n.d.	n.d.	n.d.	n.d.	
(u)		n.d.	26.47	2.29	0.10	38.98	41.22	n.d.	n.d.	0.67	0.04	0.06	n.d.	
Holling-worthite	1	33.32	n.d.	1.44	0.15	n.d.	5.30	10.47	n.d.	0.19	13.59	0.54	39.70	104.90
Polarite	1	n.d.	n.d.	2.06	n.d.	65.34	27.84	n.d.	n.d.	n.d.	n.d.	0.06	n.d.	95.35
UK1		18.87	n.d.	1.39	0.52	n.d.	3.59	48.58	n.d.	n.d.	13.96	0.34	9.54	96.91
UK2		n.d.	9.47	8.81	0.10	38.80	27.81	n.d.	n.d.	0.12	7.17	7.93	n.d.	100.25
UK3		n.d.	63.97	1.25	8.95	11.36	14.15	n.d.	n.d.	0.45	n.d.	0.07	n.d.	100.19
Melonite sample			67.00		10.60	9.30	12.70	n.d.		0.93				100.53

n.d. = not detected (l) = lower limit of range for each element (u) = upper limit of range for each element

Analytical details for electron microprobe analyses.

Qualitative analyses of PGM were carried out using a fully automated, wavelength-dispersive, 5 spectrometer CAMECA CAMEBAX SX50 electron microprobe, at the Anglo American laboratories (AARL), Johannesburg. The accelerating voltage used was 20kV, with a beam current of 20mA, measured and monitered on a Faraday cup. Counting times were 20 seconds on peak position and 10 seconds for background values, for all elements.

The standards used were synthetic PGM standards (supplied by Dr L.J. Cabri, and made available by AARL), mineral standards and pure elements.

Standards, X-ray lines and lower limits of detection (LLD) for 20s counting time.

Element	Standard	X-Ray Line	LLD (wt%)
Pt	$PtTe_2$	PtLß	0.60
Pd	PdTe	PdLα	0.08
Rh	PtRh	RhLα	not calc.
Te	$PtTe_2$	TeLα	0.07
Bi	$PdBi_2$	BiMα	0.11
As	$Pd_5(As,Sb)_2$	AsLα	0.07
Sb	$Pd_5(As,Sb)_2$	SbLα	0.07
S	FeS (Troilite)	SKα	0.02
Fe	FeS (Troilite)	FeKα	0.09
Ni	Ni (Pure)	NiKα	0.05
Cu	Cu (Pure)	CuKα	0.05
Zn	ZnS	ZnKα	0.07

0.045% Rh and 0.2% As respectively. The interference of Pt with Bi was avoided by using the Pt-$L\beta$ line instead of the Pt-$L\alpha$ line, which interferes with the Bi-$M\alpha$ line. The disadvantage of using the Pt-$L\beta$ line is the low intensity for this line.

Platinum-group mineral phases and compositions

In the 12 polished thin sections examined, 91 individual PGM grains were located and qualitatively identified using a scanning electron microscope. Of these, only 41 grains yielded satisfactory microprobe analyses; 27 grains were too small to analyse (less than 3μm in the maximum dimension in thin section), or gave unreliable analyses, and 23 grains were Au or Au–Ag alloys, on which no quantitative analyses were carried out in this study.

Thirteen different PGM phases (minerals constituted by the PGE and/or Au) were identified. These are listed in decreasing order of abundance in Table 2. Also shown are the broad mineral groups of PGM, and the relative proportions of the groups.

Three mineral grains could not be identified, although quantitative microprobe analyses were carried out. These minerals are labelled UK1, UK2 and UK3 (Table 1), and are discussed below.

Table 1 shows the most representative analysis (i.e. closest to the average) for each of the identified and unidentified PGM, as well as the range obtained for each. A detailed copy of all the analyses is available from the authors at the University of Natal, Pietermaritzburg.

The compositions of the minerals are plotted on ternary diagrams and compared with known ranges of mineral compositions reported in the literature (Fig. 4*a–e*). These show the systems: (Pt + metals)–Te–(Bi + Sb); (Pd + metals)–Te–(Bi + Sb); Pt–As–S; Pt–Pd–S; (Rh + metals)–As–S respectively.

Platinum is the most abundant element constituting the PGM, especially in the sulphide and arsenide groups. Palladium is the next most dominant PGE; the other elements make a negligible contribution to the platinum-group mineralogy as a whole, apart from Rh in hollingworthite and Ru (and minor Os and Ir) in laurite. This distribution is reflected in the relative abundance of data in each of the ternary diagrams.

Unidentified phases and complex intergrowths

Three mineral phases, labelled UK1, UK2 and UK3 (analyses shown in Table 1) could not be positively identified.

UK1. Totals for the analyses of UK1 were low, but are shown on the Pt–As–S ternary diagram (Fig. 4*c*). The mineral plots near the platarsite (PtAsS) field. The high Rh content of 9.84 wt.% (recalculated to 100% to account for low mineral total) indicates that this mineral is possibly platarsite. Cabri and Laflamme (1981) show that

TABLE 2: Platinum-Group Minerals identified, host mineral groups and relative proportions of groups.

MINERAL NAME	MIN.FORMULA	HOST GROUP			
		BISMUTHO-TELLURIDES	ARSENIDES	SULPHIDES/ SULPH-ARSENIDES	Au/Au-Ag ALLOYS
Moncheite	$PtTe_2$	X			
Sperrylite	$PtAs_2$		X		
Cooperite	PtS			X	
Braggite	(Pt,Pd)S			X	
Maslovite	PtBiTe	X			
Michenerite	PdBiTe	X			
Kotulskite	PdTe	X			
Hollingworthite	RhAsS			X	
Polarite	PdBi	X			
* Laurite	RuS_2			X	
* Au/Au-Ag alloys:					
Gold	Au				X
Electrum	Au,Ag				X
Ag-Pb-Te alloys					X
* Pt-Fe alloys					
% of total PGM		38%	18%	16%	29%
% of PGM excl. Au & Ag alloys		53%	25%	22%	

* No microprobe analyses possible due to size restrictions and/or standard unavailability.

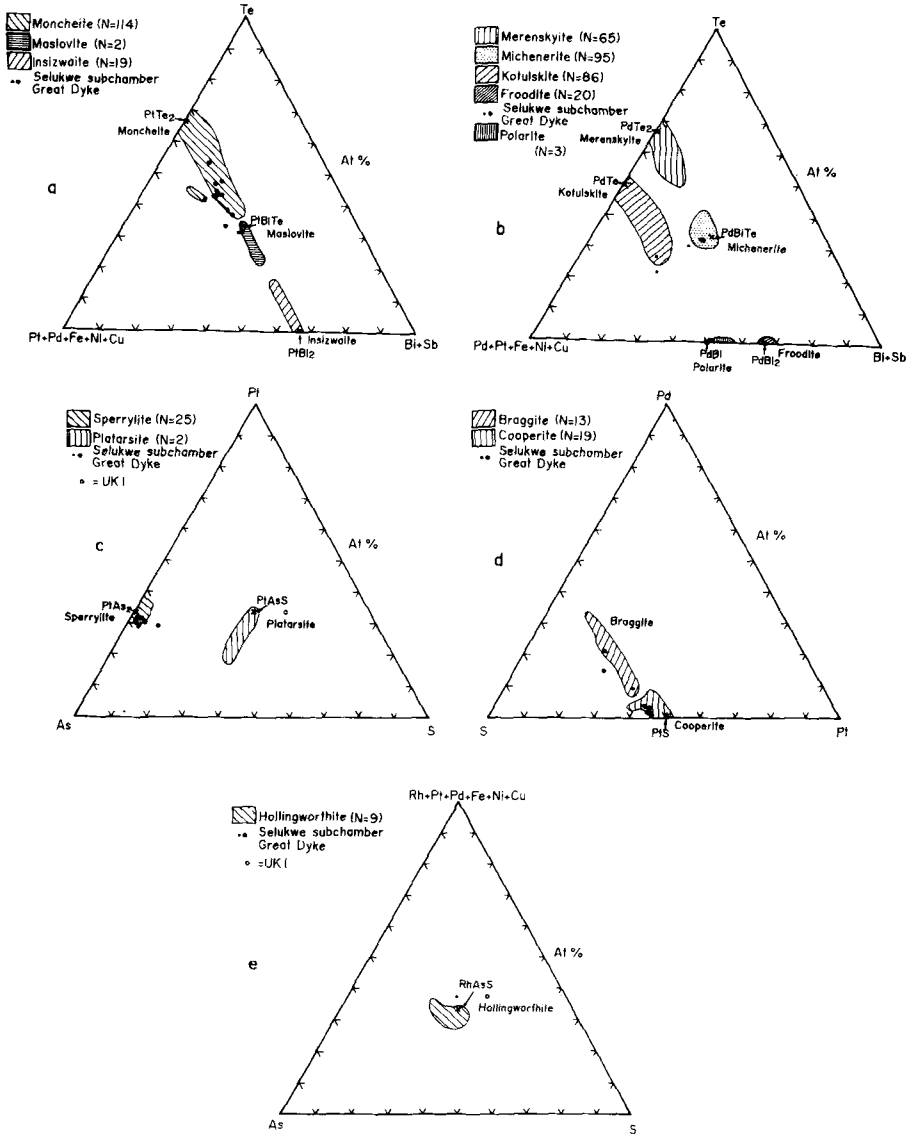

FIG. 4. Ternary diagrams showing compositions of PGM phases. The known compositional ranges, as derived from the literature, are represented by the shaded areas and include those of moncheite (114 analyses), merenskyite (65), insizwaite (19), maslovite (2), braggite (13), cooperite (19), michenerite (95), kotulskite (86), froodite (20), hollingworthite (9), sperrylite (25), polarite (3) and platarsite (2). Sources in the literature are Brynard *et al.*, 1976; Cabri and Laflamme, 1976; Cousins and Vermaak, 1976; Häkli *et al.*, 1976, Vermaak and Hendriks, 1976; Vermaak, 1976; Cabri *et al.*, 1978; 1979; Cabri and Laflamme, 1981; Beaudoin *et al.*, 1990; Harney and Merkle, 1990; Prendergast, 1990. Compositions of minerals from the study area are represented by dots—large dots for those analyses yielding weight percent totals from 98 to 102%, and small dots for those analyses with totals from 95 to 98% and 102 to 105%. (*a*) (Pt + Pd + Fe + Ni + Cu)–Te–(Bi + Sb) ternary diagram showing compositions of moncheite and maslovite from the study area. (*b*) (Pd + Pt + Fe + Ni + Cu)–Te–(Bi + Sb) ternary diagram showing compositions of kotulskite, michenerite and polarite from the study area. (*c*) Ternary diagram showing composition of sperrylite from the study area, in the system Pt–As–S. (*d*) Compositions of braggite and cooperite from the study area, shown on a Pt–Pd–S ternary diagram (*e*) (Rh + Pt + Pd + Fe + Ni + Cu)–As–S ternary diagram showing composition of hollingworthite from the study area.

platarsite can contain up to 14 wt.% Rh. The composition of UK1 plots close to the hollingworthite field on a Rh–As–S ternary diagram (Fig. 4*e*), but it is unlikely to be hollingworthite, because of the Rh content.

UK2. The high base metal (Cu, Fe) and S content of mineral UK2 (Table 1) is possibly indicative of interference from surrounding base metal sulphides, as it occurs on the boundary of a chalcopyrite grain.

UK3. The analysis of this mineral reveals a high Ni content (Table 1). Cabri and Laflamme (1981) reported that Pd can replace Ni in melonite ($NiTe_2$), as part of a continuous solid solution series. For comparitive purposes, a representative analysis of melonite is given in Table 1, and corresponds closely to that of UK3.

Four grains were identified as being intergrowths of different PGM phases. Two of these were quantitatively analysed to represent a sperrylite–braggite intergrowth (Fig. 5*a*), and a cooperite intergrown with UK1. The other two intergrowths were qualitatively analysed on the SEM and are shown to consist of a Au–Ag–Bi–Te alloy (mineral (i) in Fig. 5*b*) and a Pd–Bi–Ti alloy (mineral (ii) in Fig. 5*b*), and a Pd–Bi–Te and Pd–As–Te intergrowth.

Mineralogical and textural relationships

Mineral textures. There are essentially three types of environment in which the PGM occur, each with associated textural features. These are summarised in Table 3, together with references to figures illustrating the textures. An important observation is that the morphology of the PGM in each of the textural types is strongly controlled by the local mineralogical environment.

The PGM are rarely enclosed in plagioclase or in contact with plagioclase, and the main silicate associations are pyroxenes and hydrosilicates. The BMS associated with the PGM are predominantly pyrrhotite and chalcopyrite, and rarely pentlandite. There does not appear to be a specific association of PGM with any particular BMS mineral type.

The sulphide group of PGM (cooperite, braggite, laurite) occurs dominantly at the silicate–sulphide boundary of sulphide inclusions within cumulus orthopyroxene grains, and are nearly always in contact with unaltered pyroxene.

Sperrylite minerals (arsenide group) occur as two groups related to position in the sequence and local environment. The first (Type 1 sperrylite) is represented by large, equidimensional grains, occurring most commonly on the boundary between sulphides and altered orthopyroxene. These grains have a clearly-defined euhedral form in the sulphide grains, and are very irregular where they extend into silicates. They occur most commonly in the lower ore zone. The second group (Type 2 sperrylite) is characterised by small, typically elongate and irregularly-shaped grains occurring predominantly in the upper parts of the mineralised zone. These sperrylites are mostly found wholly enclosed in hydrosilicate minerals, and only rarely are small fragments of sulphide attached to them or occur in close proximity.

The bismuthotelluride group of PGM occurs in the same environments as Type 2 sperrylites in that they are seldom in contact with unaltered pyroxene.

Gold, electrum and other Au alloys are predominatly silicate-hosted, occurring in the interstices between pyroxene grains, but often in the proximity of pyrite or pyrrhotite.

In general, the PGM predominantly occur as individual single mineral grains; however, the bismuthotelluride group occasionally occurs as clusters of grains of the same or different phases. Type 2 sperrylite also occurs as clusters with bismuthotellurides, but none of the sulphide group of PGM have been found in this association. The sulphide PGM may occasionally cluster with Type 1 sperrylite or other sulphides. Au and Au alloys are found only as single grains or as rare, small clusters.

Relationship between textural environment and mineral composition. Except for sperrylite and moncheite, there are insufficient analyses of PGM to unequivocally correlate compositional variations within the different minerals to the local textural environments.

Sperrylite shows no particular mineral compositional trends related to textural environment, but it is noticeable that those grains which are wholly enclosed in hydrosilicates have a very narrow compositional range. Moncheite grains which are wholly enclosed in hydrosilicates are Pt- and (Bi + Sb)-depleted, and Te-enriched, compared with the minerals in other environments (Fig. 6).

Both moncheite and sperrylite grains enclosed wholly in hydrosilicates have higher Sb values than the grains in other environments. Moncheite enclosed in hydrosilicates has Sb contents ranging from 0.41–0.63 wt%, compared with 0.23–0.39 wt.% of the element for the mineral in other environments. Type 2 sperrylites enclosed only in hydrosilicates have Sb contents in the 0.30–0.35 wt.% range, whereas for Type 1 sperrylite the values range from 0.00–0.20 wt.%. This indicates that the formation of hydrosilicates took place at a relatively late stage and was associated

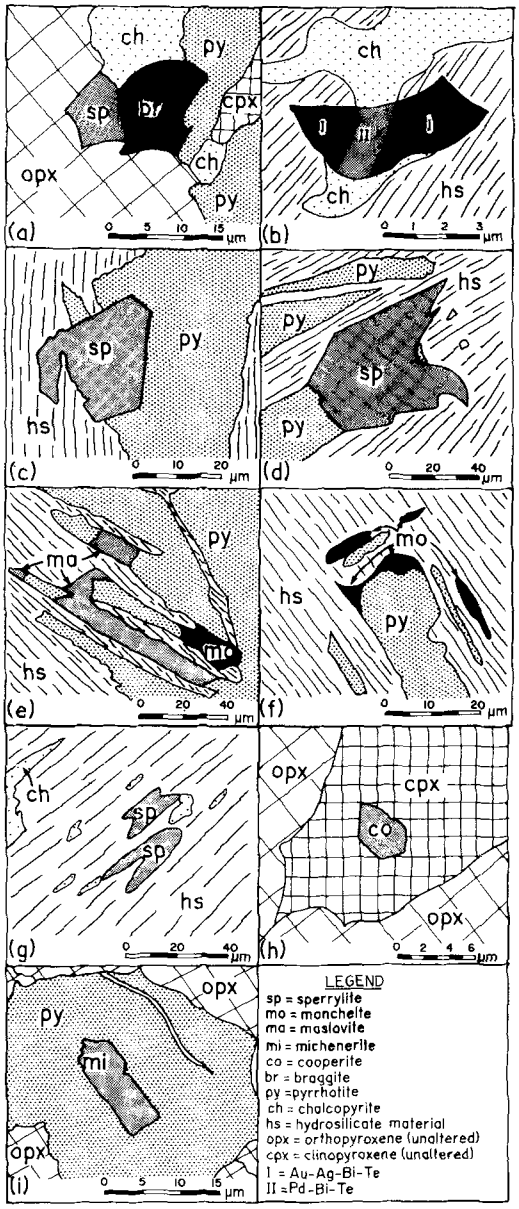

FIG. 5. Characteristic textural forms of the Great Dyke PGM: (*a*) Sperrylite-braggite intergrowth on orthopyroxene-sulphide boundary. (*b*) Intergrowth of Au–Ag–Bi–Te alloy (i) with Pd–Bi–Te alloy (ii), hosted by sulphide and hydrosilicate. (*c*) Sperrylite grain exhibiting euhedral form in sulphide and irregular form in hydrosilicate. (*d*) Large sperrylite grain 'attached' to edge of sulphide grain and intergrown with hydrosilicate. (*e*) Maslovite and moncheite showing apparent restriction to sulphide boundaries with 'corrosion' textures. (*f*) Moncheite defining the edge of a sulphide grain ('corrosion' texture); other grains wholly enclosed in hydrosilicate. (*g*) Highly irregular sperrylite grains, with minor sulphide grains attached to them, wholly enclosed in hydrosilicate. (*h*) Subhedral cooperite grain wholly enclosed in unaltered clinopyroxene. (*i*) Subhedral michenerite grain wholly enclosed in pyrrhotite.

with redistribution of low-temperature components.

PGM grain sizes. Grain sizes of the PGM were determined in section by measuring the length of

TABLE 3: Environments and textures of the PGM.

ENVIRONMENT DESCRIPTION	% PGM IN ENVIRONMENT	EXAMPLES OF TEXTURAL FEATURES SPECIFIC TO ENVIRONMENT
1) PGM on base-metal sulphide (BMS) - silicate mineral boundary (silicates may be primary magmatic pyroxenes or plagioclase, or secondary hydrated/altered phases).	57%	a) **Fig.5(c)**: PGM intergrown into both silicate and sulphide hosts, being euhedral in form against the sulphide and irregular where extending into the silicate. Common for larger sperrylite grains. b) **Fig.5(d)**: PGM in contact with, but not intergrown with, the sulphide edge, and extending into silicate matrix. c) "Corrosion" texture: growth of the PGM is restricted to the BMS boundary, or corroded to the boundary. Common for bismuthotellurides and smaller sperrylite grains. **Fig.5(e)**: PGM appear to have replaced part of the sulphide grains. **Fig.5(f)**: PGM occur as clusters at inside edge of sulphide grain.
2) PGM hosted entirely in silicates (usually in close proximity to BMS).	34%	a) **Fig.5(g)**: PGM may be elongate & subhedral in form, to highly irregular, in hydrated silicates. b) **Fig.5(h)**: PGM may be rounded to subhedral in unaltered pyroxenes.
3) PGM wholly enclosed in BMS.	9%	a) **Fig.5(i)**: PGM euhedral, to subhedral or rounded.

the longest axis and that perpendicular to the longest axis (data summarised in Table 4). Grains having a measured dimension <4μm were not analysed quantitatively using the microprobe, but in most cases the mineral type was identified qualitatively using the SEM and those data are included in the size analysis.

A size histogram, expressed in terms of the longest axis for each mineral type, is shown in Fig. 7. Each mineral type exhibits a range of sizes, but sperrylite, in general, is the coarsest-grained mineral. Half of the population of this mineral type has long axes >15μm, but there is a complete range in sizes, to as small as 2μm in the longest dimension. The sperrylites comprise two distinct size groups, one group being characterised by

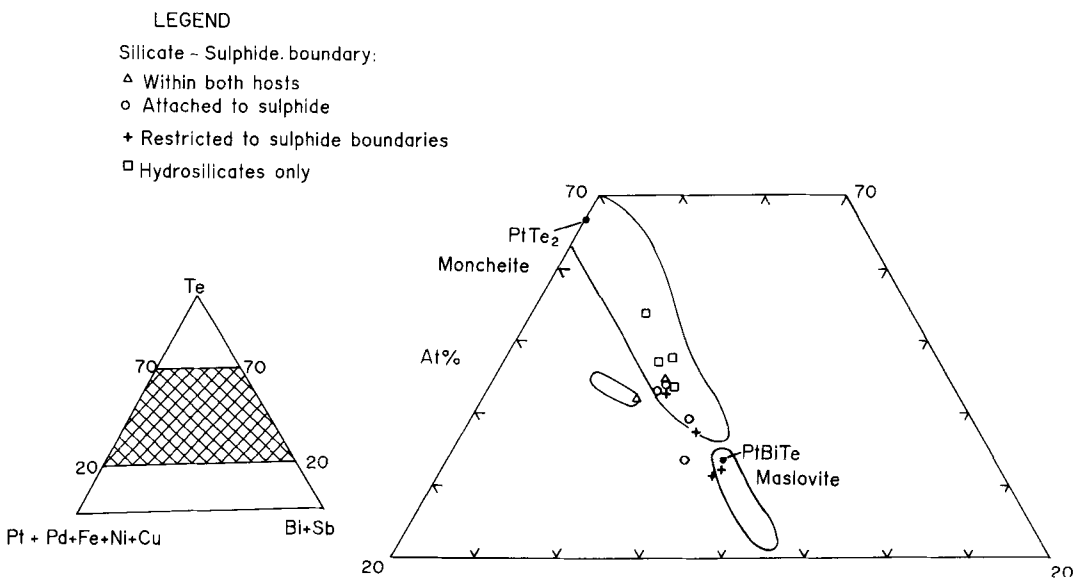

FIG. 6. (Pt + Pd + Fe + Ni + Cu)–Te–(Bi + Sb) ternary diagram showing grouping of those moncheite grains variably enclosed in hydrosilicates and sulphides.

TABLE 4: Size statistics of PGM

Long axis		Shorter axis (90° to long)	
Range: 2-82 μm		Range 1-50 μm	
Interval (μm)	% PGM	Interval (μm)	% PGM
<4	10	<4	42
4-15	70	4-10	49
>15	20	>10	9

relatively large (>20 μm) and generally equidimensional grains, the other group being in the size range of 5 to 10 μm in length. The grains of the sulphide PGM group are smaller than those of the sperrylite group, and are generally restricted to the 3–10 μm range. The bismuthotellurides exhibit a wide range of sizes, between 3 and 20 μm. Electrum, native gold and Au alloys are relatively coarse-grained, with long axes ranging from 5 to 40 μm.

Stratigraphic distribution of PGM through the mineralised zone. The distribution of PGM within the vertical profile is expressed as grain frequency with stratigraphic height for the different PGM (Fig. 8*a*), and volume distribution with stratigraphic height (Fig. 8*b*). The approximate volumes were calculated by assuming the PGM to be regular in shape and using areas calculated from the size measurements.

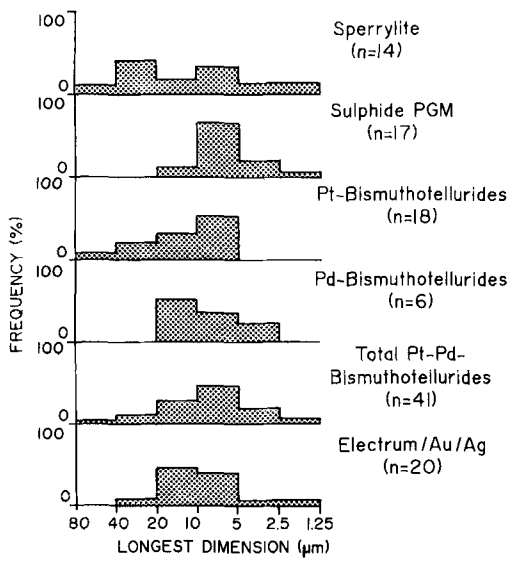

FIG. 7. Histogram showing distribution of sizes for the various PGM. The sulphide PGM include braggite, cooperite, laurite and hollingworthite; Pt-bismuthotellurides include moncheite and maslovite; Pd-bismuthotellurides include polarite, kotulskite and michenerite; total Pt–Pd–bismuthotellurides include all qualitatively and quantitatively identified Pt–Pd–bismuthotellurides.

Sperrylite occurs throughout the Main Sulphide Zone (note change in scale between MSZ and LSZ in Fig. 8*a* and *b*). The grain frequency plot shows it to be most abundant in the upper parts of the zone. However, the volume distribution of sperrylite indicates it to be in greatest abundance at the base of the zone. Type 1 sperrrylites comprise the larger, equidimensional grains predominant in the lower MSZ, and these grains account for the observed volume distribution. The smaller Type 2 sperrylites are those intergrown with hydrosilicates in the upper MSZ. Both the frequency and volume plots show that the sulphide PGM group is stratigraphically intermediate to the lowest sperrylite population and the bismuthotellurides. Although the bismuthotellurides occur throughout the MSZ, they are dominant in the upper parts, coincident with, and just below, the uppermost sperrylite population. Au and Ag alloys are most abundant in the highest part of the zone.

In the Lower Sulphide Zone, the sulphide PGM dominate the lowest part of the zone, whereas the sperrylite and bismuthotelluride PGM only appear at the very top of the zone. Au alloys show a predominance at a stratigraphic position intermediate to that of sperrylite and the bismuthotellurides.

Discussion

The silicate framework to the Great Dyke PGE deposits. The formation and postcumulus development of the P1 layer, in particular the sulphide zones, plays an important part in understanding the origin of the PGE deposits, the PGM distribution and their textures.

Cyclic Unit 1 formed as the result of a major impulse of new magma. It is characterised by economic chromitite layers at its base, with olivine the dominant cumulus phase in the lower units, being joined by cumulus bronzite higher in the sequence. Repeated minor magma influxes resulted in repetition of stratigraphy. The P1 layer represents the point at which bronzite became the dominant cumulus phase (Wilson, 1982; Wilson and Prendergast, 1989; Prendergast and Wilson, 1989; Wilson, 1992).

Formation of P1 thus commenced with nucleation and subsequent growth of cumulus bronzite crystals in equilibrium with the main body of magma. Clinopyroxene and plagioclase formed postcumulus oikocrysts, initially as heteradcumulus phases which were later enlarged by over-

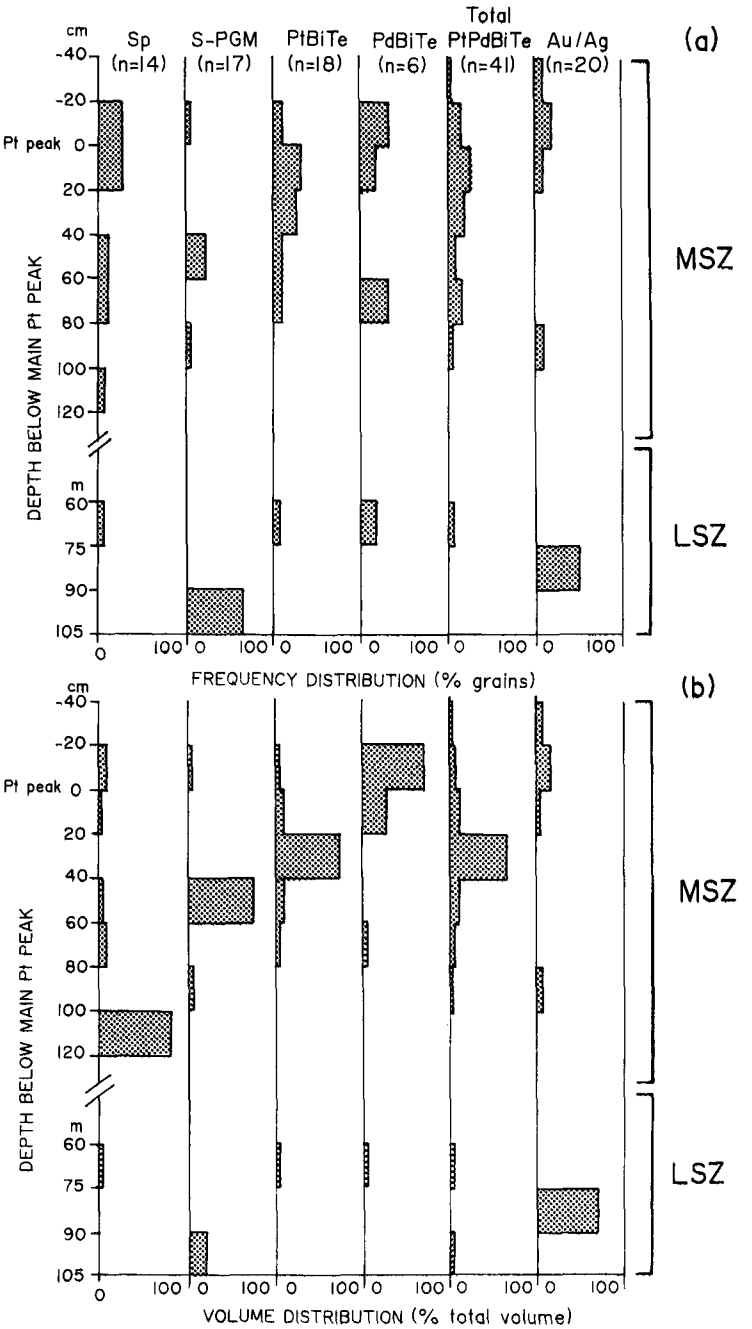

FIG. 8. Histograms showing vertical distribution for the various PGM in terms of (*a*) grain frequency and (*b*) volume. Depths are given relative to the main platinum peak of the MSZ. Note the change in scale between the MSZ and LSZ—those depths in cm represent the MSZ and those in m, the LSZ. Sp = sperrylite; S–PGM = sulphide PGM group; PtBiTe = Pt–bismuthotellurides; PdBiTe = Pd–bismuthotellurides; Total PtPdBiTe = Total Pt–Pd–bismuthotellurides; Au/Ag = Electrum and Au alloys.

growth from the trapped liquid. The formation of immiscible sulphide droplets would have occurred at this point, assuming a state of sulphur-saturation in the magma. With continued growth of the oikocrysts, intercumulus liquids and sulphide liquids became trapped and distributed around the oikocrysts, the system eventually becoming closed with respect to the main body of magma. The trapped intercumulus liquids crystallised separate crystals of postcumulus clinopyroxene, and the remaining highly evolved liquid formed the late-stage (high temperature) mineral assemblage of phlogopite, quartz, K-feldspar, hornblende and talc. Solidification of sulphide liquid completed the primary development of P1 (Wilson, 1992).

During crystallisation of the late-stage assemblage, a hydrous, volatile phase was released and reacted with the sulphides to produce a reactive acidic fluid. This highly corrosive fluid reacted with primary silicates resulting in replacement of low-temperature hydrosilicate assemblages of talc, amphiboles, chlorite and secondary magnetite, i.e. a process of deuteric alteration occurred (Prendergast, 1990). Redistribution of sulphide and PGE by the late-stage volatiles occurred, as well as intergrowth of hydrosilcates and sulphides, resulting in the characteristic alteration and intergrowth textures observed in the sulphide zones. The implications for the PGM are discussed in a later section.

The magmatic origin of PGE deposits. The close association of PGE with sulphides in many layered intrusions [for example, the MSZ of the Great Dyke, the Merensky Reef (Bushveld Igneous Complex), Munni Munni Complex, J–M Reef (Stillwater Igneous Complex)] indicates that liquid sulphide acted as a collector for these metals. Campbell *et al.* (1983) proposed that the PGE were scavenged from the silicate magma by an immiscible sulphide melt which segregated at a point of sulphur saturation in the magma. The Nernst distribution coefficients required for such a process are proposed by Campbell *et al.* (op. cit.) and Campbell and Barnes (1984) to have very high values, as high as 10^5. Each PGE may have had a slightly different value for the distribution coefficient, which is reflected in the relative displacement of the individual PGE peaks and the base metal sulphide peak, for the Great Dyke (Prendergast and Keays, 1989; Wilson and Tredoux, 1990) and also for the Munni Munni Complex (Barnes *et al.*, 1990).

For the formation of an economic sulphide-hosted PGE deposit, enrichment factors for a normal basaltic magma are required to be in the order of about 10^3 (Macdonald, 1987). High distribution coefficients alone are insufficient to account for the enrichments seen in PGE deposits. Campbell and Naldrett (1979) introduced the concept of the R-factor, which expresses the ratio of the mass of host magma to sulphide liquid necessary to produce this enrichment. In order for the scavenging process to be sufficiently effective to result in an economic deposit, sulphide droplets must come into contact with a large volume of silicate magma.

Mixing and turbulence in a magma, often associated with new magma impulses, are the dominant control in achieving a high R factor (Campbell *et al.*, 1983). The fluid dynamics of a magma are affected by chamber geometry and by differences in temperature, composition, viscosity and density within the magma, or between a resident magma and a new impulse (Campbell *et al.*, 1983). The general occurrence of PGE-rich sulphide horizons at or near the bases of cyclic units, which are indicative of a new magma impulse, imply that their genesis is linked to new injections of magma.

The formation of an economic PGE deposit is dependent on the subsequent accumulation of the sulphide as an immiscible phase. For sulphide liquation to occur, the silicate liquid must become sulphur saturated (Naldrett *et al.*, 1990). The factors affecting sulphur solubility are temperature, oxygen fugacity, changes in magma composition (due to fractionation or assimilation of country rock) and mixing of two or more disparate magmas (Haughton *et al.*, 1974; Buchanan, 1988).

In accordance with a magmatic origin, the LSZ and MSZ represent stages in the crystallisation of Cyclic Unit 1 at which sulphide liquation, and hence PGE scavenging, occurred. The disseminated, sparsely mineralised LSZ owes its formation to low volume segregation of sulphide, with saturation having been achieved by decreasing temperature and increasing S-content due to fractional crystallisation of the magma (Wilson *et al.*, 1989; Naldrett *et al.*, 1990). The greater mass of sulphide in the MSZ resulted from the mixing of resident magma with an evolved magma originating higher in the chamber, possibly due to plagioclase crystallisation, producing a hybrid magma which was driven strongly into the sulphide saturation field (Naldrett and Wilson, 1989; 1990). Progressive mixing caused fractional segregation of sulphide over a narrow vertical interval.

The hydrothermal origin of PGE deposits. There is considerable evidence to support the origin of PGE deposits in layered intrusions as the result of post-liquidus deuteric processes. The evidence includes the association of PGM with

hydrous silicate phases and altered primary silicates, increased amounts of graphite and chlorite and textures indicative of recrystallization (pegmatoids) and movement of fluid (Balhaus and Stumpfl, 1986; Stumpfl and Balhaus, 1986; Boudreau, 1988). Most models involve complexation of PGE with a Cl-rich fluid which is capable of transporting the metals to the zone of concentration, notably the sulphide-rich layer. The fluid phase is generated by exsolution from an evolved intercumulus silicate liquid in the final stages of differentiation, which is then expelled upwards through the pile of cumulus mineral grains. Boudreau *et al.* (1986) show that a process which is akin to zone refining will progressively enrich the fluids as they move up through the crystal pile and encounter pockets of liquid that had not yet reached saturation of halogens. Precipitation of PGM occurs along the boundaries of sulphide grains from the Cl-rich solutions.

Evidence to support this mechanism is the observed distribution of PGM around sulphide grains and the hydrous nature of the associated silicates. In the J–M Reef of the Stillwater Complex, evidence cited to support a hydrothermal origin of the mineralisation is the high degree of variability of the reef and the lack of continuity over a scale of metres to tens of metres (Raedeke and Vian, 1986).

In contrast to the J–M Reef, the MSZ of the Great Dyke is persistent as a continuous tabular body over hundreds of kilometres (where exposure of the P1 layer at the appropriate level is preserved), and is remarkably homogeneous over a scale of tens to hundreds of metres, with the only observable variation reflecting gradation in its environment from axis to margin (Wilson and Prendergast, 1989; Naldrett and Wilson, 1990; Wilson and Tredoux, 1990; Prendergast, 1991).

In addition, the form of the PGE distribution in the Great Dyke ore zone is one of an ascending series of peaks through the vertical profile, these peaks bearing a strong linear proportionality to each other (Wilson and Tredoux, 1990). It would be highly improbable for this complex pattern to be preserved over many kilometres by a process of PGE mineralisation that required mass transport, such as fluid migration, which by its very nature would impose a high degree of variability. Furthermore, the offset distribution of the different PGE through the vertical profile, which is a feature of the Great Dyke deposit (Prendergast and Keays, 1989; Wilson and Tredoux, 1990), is also highly unlikely to have been derived from a primary hydrothermal-type process. Similar characteristics are also found in the PGE zone of the Munni Munni complex and early magmatic processes rather than fluid migration are considered to be the controlling mechanism (Barnes, *et al.*, 1990).

The style of alteration, the nature of the PGM assemblage and its relationship to the base metal sulphides, are indicative of the active involvement of fluids in the ore zone, but, as will be shown in the next section, this can be explained largely as the result of the highly reactive fluid phase generated by the differentiation of intercumulus liquid within the ore zone, rather than by the introduction of external components.

The role of complexation and intermediate compound formation in the genesis of the Great Dyke PGE deposits: a multi-process model. One of the chemical features of the PGE is their ability to readily undergo complex compound formation in a wide range of environments, from early magmatic to late-stage hydrothermal. In most cases, the processes leading to the formation of these compounds are obscure, because the observed PGM assemblage invariably bears little resemblance to the original, or even the intermediate compounds. Several points need to be considered in establising the genetic pathways of the Great Dyke PGE ore deposits. These are: (1) the broad association of PGE with base metal sulphides indicates that the formation of sulphides was crucial to the enrichment process; (2) many of the textural types indicate that the PGM eventually became isolated or detached from the sulphide; (3) the zone of PGE enrichment is associated with an enhanced level of semi-metals (Sb, Te, As, Bi); arsenide and bismuthotelluride PGM characterise the assemblage, but minerals containing Bi, Te, Pb and As are absent in the PGE-deficient parts of the MSZ; and (4) the PGM show a wide range of thermal stabilities, from what appear to be isolated primary high temperature mineral phases of magmatic origin, to low temperature phases consistent with a hydrothermal origin.

Even at high temperatures there is a complex association between iron sulphides and PGE sulphides. Cooperite (PtS) coexists in stable relationship with pyrrhotite at 1000 °C (Skinner *et al.*, 1976), whereas braggite (PdS) is stable with S-rich pyrrhotite only below 900 °C (Makovicky *et al.*, 1990). Platinum arsenide (sperrylite group) has a wide range of stabilities, and may co-exist with melts of widely different composition.

It is commonly assumed that PGE partition into sulphides at high temperature, on the basis of their forming complete solid solution with liquid base metal sulphides. Although this may be true in part, it is probably an oversimplification. Palladium shows strong chalcophile character,

whereas the other elements are dominantly siderophile. This indicates that no one single mechanism is capable of explaining the enrichment of the group. For instance, Ir may be incorporated in early-formed high temperature silicate minerals (Davies and Tredoux, 1985), but the element is also strongly enriched with other PGE in the sulphide zone. It is also apparent that distribution coefficients determined from experiment and in natural systems encompass a very wide range in values (e.g. Barnes and Naldrett, 1985; Peach *et al.*, 1989). As noted previously, the distribution coefficient for Pt between sulphide and silicate liquid ranges from 2000 (Campbell and Naldrett, 1979) to nearly 200 000 (Campbell and Barnes, 1984). Helz (1985) shows that Pt and Pd are strongly siderophile at magmatic temperatures (1200 °C), and although these elements may be associated with high temperature sulphide melts, PGE sulphide minerals as discrete species are not stable. Helz (op. cit.) suggests that these elements occur in elemental form more as colloids than as cationic species.

Lindsay (1988) reconciles many of these observations in a mechanism which invokes the coalescence of PGE atoms to form metastable molecular clusters, rather than their complete solution in liquid sulphide. These clusters are stabilised by S and the group of semi-metals As, Te and Bi, which are then easily incorporated into monosulphide solid solution. The clusters may form proto-PGM in the sulphide, or become trapped in the monosulphide solid solution. This early association of sulphide and stabilised PGM clusters is based on physical rather than chemical properties, which is likely to give a wide range of apparent distribution coefficients, depending on composition of the melt, temperature, oxygen fugacity and path followed in the formation of the metastable compounds.

The base metal sulphides in the Great Dyke (and those in most other PGE-enriched zones in layered instrusions) contain only small amounts of PGE, and therefore these elements must have been expelled during the cooling process. The discrete mineral phases observed in this study indicate that considerable redistribution of the PGE and semi-metals took place following their exclusion from the sulphide, and prior to their crystallisation as low-temperature phases. It is suggested that following expulsion from sulphide, local redistribution of the PGE and the dissociated suit of semi-metals took place in the highly reactive fluid phase resulting from the fractionation of trapped intercumulus liquid. The semi-metals and PGE reached critical concentrations and proportions, initiating crystallisation and growth of low temperature PGM.

An alternative argument may be that arsenic may reach saturation in the magma and therefore scavenge PGE in the same way that sulphide is proposed to do; however, this would result in some deposits being generally As-enriched, with only weak development of sulphide mineralisation. There are no such examples in layered intrusions, and in the case of the Great Dyke, the mineralisation is coincident with the onset of sulphide formation. The presence of the semi-metals is critical to the early entrapment process of the PGE, as well as to their ultimate low temperature reassociation.

The series of complexation processes shown in Fig. 9 indicates that the incorporation of PGE into sulphide from silicate magma is dependent on both the sequence of events as well as efficiency of each part of the process. It is therefore unlikely that a unique value could express the apparent distribution coefficient of an individual PGE between silicate and sulphide liquids. In spite of this limitation, the effectiveness of the incorporation of PGE into early-formed sulphide is useful in modelling the vertical distributions of PGE (Wilson and Tredoux, 1990; Barnes *et al.*, 1990), and therefore in a paticular environment this may be expressed as real value. We suggest use of the term 'Affinity Factor', which is expressed in the same way as distribution coefficient, but does not carry the implications required of a chemically coherent system, as being appropriate to describe the influence of sulphide in the magmatic development of a sulphide-hosted PGE deposit.

On the basis of the approach used here, the PGM assemblage in the Great Dyke ore zone may be broadly divided into the early stage (orthomagmatic) and late stage (hydromagmatic).

Orthomagmatic PGM assemblage. The sulphide group of PGM (hollingworthite, laurite, cooperite and braggite), as well as platinum arsenides of the Type 1 sperrylites, fall into this category. These are high-temperature minerals forming early in the crystallisation history, which accounts for their spatial distribution in the vertical profile in that they are concentrated near the base of the MSZ ore zone. The sulphide phases probably crystallised rapidly as very small grains nucleating on growing pyroxene crystals, which then enclosed the grains, or were subsequently incorporated into sulphide droplets as these coalesced. Sulphide PGM enclosed within the pyroxene were preserved as discrete mineral grains and protected from interaction with the fluid phase which developed later. This group of

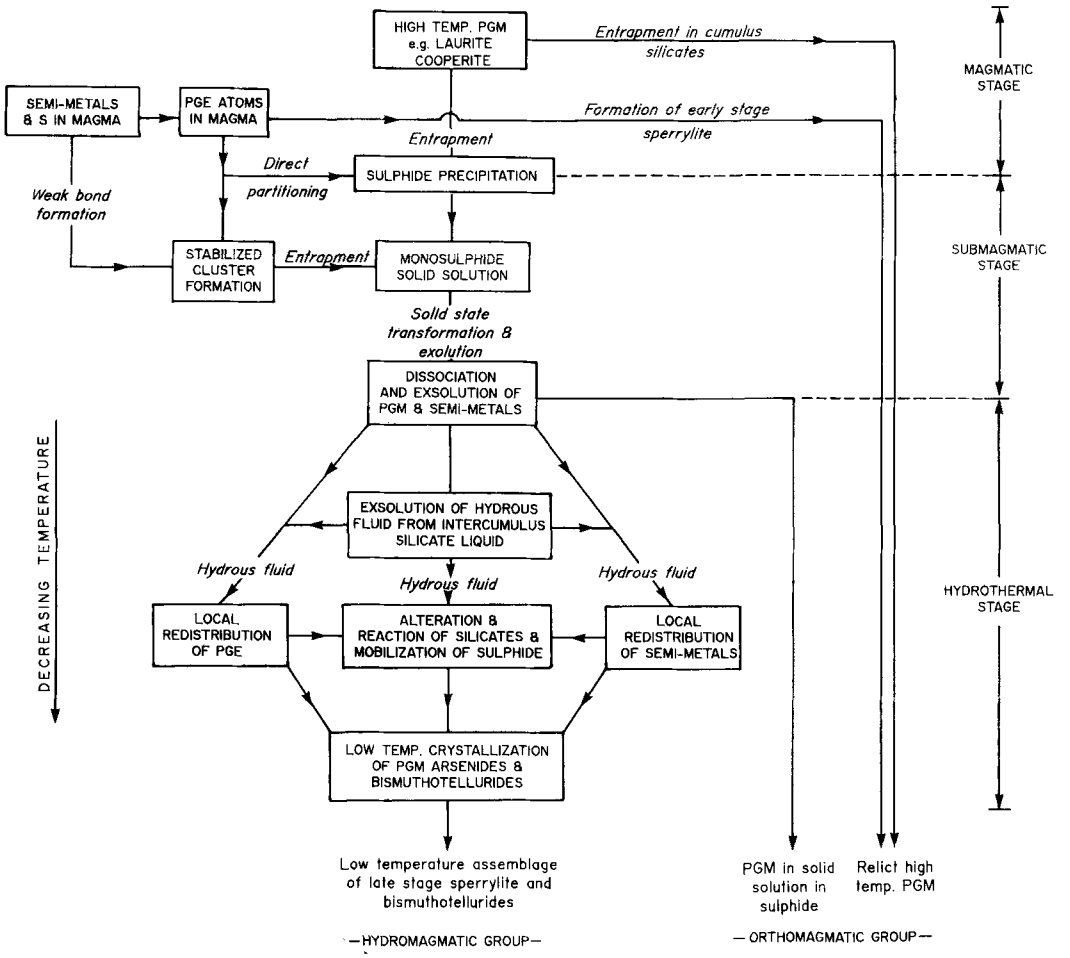

FIG. 9. Proposed sequence of events showing the multi-process model for the genesis of PGM in the Great Dyke. The definitive stages are high-temperature early magmatic, through submagmatic, to low-temperature late-stage hydromagmatic.

high-temperature minerals is relatively small and comprises a minor proportion of the total PGM assemblage, because the tendency would be for these to have been incorporated into sulphide with only rare crystals trapped in cumulus pyroxene.

Platinum arsenide (Type 1 sperrylites) formed as part of the high-temperature assemblage, this mineral having a wide stability range. This mineral may also have been activated by S and adhered to the boundary of sulphide droplets along linear grain boundries, but continued to grow even at very low temperatures by interaction with late-stage fluids, causing the boundary, which was in contact with the hydrosilicates, to be irregular. This textural relationship does not imply that hydrous silicate phases pre-dated the solidification of sulphide, as suggested by Prendergast (1990).

Hydromagmatic PGM asssemblage. The bismuthotellurides, the Type 2 sperrylite grains and overgrowth on the orthomagmatic generation of sperrylite comprise the late-stage hydromagmatic assemblage of PGM. These minerals are always in contact with or enclosed in hydrosilicates and highly altered pyroxenes, and occur predominantly in the upper part of the mineralised zone, together with higher sulphide content and generally more intense alteration. During the alteration process, hydration and replacement of primary silicates took place, with the formation of biotite, several minerals of the amphibole group and talc. The alteration, although pervasive, is variable on a small scale and is controlled by the local

distribution of liquid sulphide, as well as the concentration of extreme differentiates of trapped late-stage fluid. This distribution is linked to the development of oikocryst phases as controlling the formation of the nodular pyroxenite (Wilson, 1992). The liquid sulphide accumulated in the porous regions of the network formed by the cumulus pyroxenes, and these would also have been the regions of concentration of the final late-stage fluids. Cumulus pyroxenes which occur as a close network or enclosed in the early-stage portion of oikocrysts, are much less altered, which also indicates that the alteration process is of a local nature and does not result from the widespread and pervasive migration of hydrothermal fluids. The sulphide originated as a primary liquid (of cumulus status), but was displaced over short distances by the growing oikocrysts of clinopyroxene and plagioclase, as well as by the postcumulus overgrowth of cumulus orthopyroxene. As a result of this process, the sulphide liquid was in close contact with the pockets of late-stage hydrous fluid.

As the activity of the hydrous fluid increased, reaction with sulphide, both in the remnant liquid stage and as solid sulphide, took place to produce a highly acidic fluid. Iron was released from the sulphide, which, together with the local high concentration of potassium, initiated the formation of biotite, which is seen to replace sulphide. The reactive acidic fluid caused leaching of the pyroxene where these grains were in contact with the fluid, and along cleavage planes, resulting in replacement by talc and fibrous amphiboles. Release of Fe both from the pyroxene and the sulphide resulted in the formation of magnetite as trains within pyroxene cleavages, as well as within the hydrous mineral assemblage. At the same time that this alteration process was taking place, PGE were remobilised within the pockets of fluid and crystallised to give the suite of low-temperature PGM. Some of these even migrated along pyroxene cleavages.

The reactivity and pervasiveness of the alteration would have been dependent on the amount of sulphide in the rock, and therefore the degree of alteration and formation of hydrous phases can also be related to the proportion of sulphide. This is particularly noticeable because of the fact that the alteration commences at the first appearance of sulphide and increases markedly upwards in the ore zone.

In the same way, local migration of the highly volatile semi-metals (Te, Bi and As) moving along narrow passageways within the hot crystal pile, would in some parts have corroded early-formed arsenides and bismuthotellurides protruding from sulphides (producing the observed 'corrosion' textures) and deposited these components as late-stage minerals within the hydrosilicate assemblage. In view of this, there is a general zonal effect of the PGM on a small scale through the vertical profile, together with the establishment of the second generation of sperrylites. Those PGM entirely enclosed within either sulphides or early-formed silicates, would effectively have been shielded from the hydrothermal processes which operated on a local scale.

The complex multi-process origin proposed for the Great Dyke PGE deposits has implications for other layered intrusions. Evidence for the modification of primary textures by a continuum of post-magmatic processes, indicates that all PGE deposits in layered intrusions must have undergone these processes to some degree. In a detailed study of the elements As, Bi, Hg, S, Sb, Sn and Te in the J-M Reef of the Stillwater Complex, Zientek *et al.* (1990) conclude that neither liquidus processes nor fluid migration explain the observed distribution of these elements. Zientek *et al.* (op. cit.) show that elemental abundances and ratios are different in the mineralised and unmineralised parts of the sulphide zone. Such observations are entirely consistent with the mechanisms proposed for the Great Dyke in that these elements played a critical role in the initial precipitation of the PGE and were subsequently retained in the local environment.

These conclusions also have implications for the exploration of PGE in ultramafic rocks. Elements such as arsenic at low parts per million level would be easier and less costly to analyse using routine analytical techniques (such as XRF) than would be PGE, and anomalies of semi-metals may be used as indicators of Great Dyke-type mineralisation processes.

Conclusion

The characteristics of the PGM documented in this study point to both orthomagmatic and hydromagmatic processes having contributed to the final product of mineralisation. The most important of these features are: (1) the stratigraphic distribution of the different PGM, *viz.* high-temperature PGM (hollingworthite, laurite, cooperite, braggite and Type 1 sperrylite) dominating the lower parts of an ore zone, and low-temperature PGM (Type 2 sperrylite and bismuthotellurides) being more abundant in the higher regions; (2) the different textural environments in which the PGM occur, *viz.* being wholly enclosed in either sulphides or silicates, or more commonly, being situated on the boundary of

sulphide and silicate (or hydrosilicate) minerals; (3) the textural features characteristic of the PGM, especially of those in the sulphide–silicate boundary environment, *viz.* the PGM grown into both the sulphide and silicate hosts, the PGM attached to sulphide and extending into the silicate, and 'corrosion' textures; (4) the strong relationship between the size of the PGM, their compositions, mineral associations and spatial occurrence.

The general conclusion that can be drawn is that initiation of sulphide mineralisation, subsequent early local concentration of PGE, and nucleation and primary development of the high-temperature PGM assemblage were due to orthomagmatic processes.

There is no evidence to suggest that PGE were introduced to the system by a fluid phase. However, fluids are considered to have played an important role in the subliquidus stage and the formation of the low-temperature assemblage of PGM, and were responsible for remobilisation of PGE and PGM components on a local scale.

The association of PGM with the semi-metals (As, Bi, Te, Sb), indicates that these were significant in stabilising the PGE at a late-stage, and possibly even played a role in the complexation process at high temperature.

Use of the term 'Affinity Factor' is proposed to express the apparent distribution coefficient of an individual PGE between silicate and sulphide liquids. This factor will be dependent on the particular environment, sequence of complexation processes and efficiency of the processes.

Although magmatic processes controlled the initial PGE enrichment, and on this basis the stratiform, sulphide-hosted PGE mineralisation of the LSZ and MSZ can be classified as orthomagmatic in origin, it was the postcumulus development and consolidation of the sulphide-rich zones which were responsible for most of the observed characteristics of the PGM.

The proposed multi-process model for the petrogenesis of the Great Dyke PGE deposits has implications for sulphide-hosted PGE deposits in other layered intrusions.

Acknowledgements

This paper results from Ph.D. studies by BMC, supported by Anglo American Corporation, Zimbabwe. AACZ is thanked for permission to publish this paper in particular Prof. K. Viewing is thanked for making borehole core available for the study, and for generous support in all facets of the project. BMC acknowledges the Foundation for Reseach Development (FRD) for the award of a postgraduate bursary and a studentship. AHW acknowledges FRD for funding to support travel and laboratory expenses. Mr R. Corrans of Anglo American Corporation (South Africa) is thanked for funding the microprobe study, which was carried out at the Anglo American Research Laboratory at Crown Mines, Johannesburg. Great assistance at the laboratory was given by Dr H. Horsch.

References

Balhaus, C. G. and Stumpfl, E. F. (1986) Sulphide and platinum mineralisation in the Merensky Reef: evidence from hydrous silicates and fluid inlcusions. *Contrib. Mineral. Petrol.*, **94**, 193–204.

Barnes, S. J. and Naldrett, A. J. (1985) Geochemistry of the J-M (Howland) Reef of the Stillwater Complex, Minneapolis Adit area. I. Sulfide chemistry and sulfide–olivine equilibrium. *Econ. Geol.* **80**, 627–45.

Barnes, S. J., McIntyre, J. R., Nisbet, B. W., and Williams, C. R. (1990) Platinum Group Element Mineralisation in the Munni Munni Complex, Western Australia. *Contrib. Mineral. Petrol.*, **42**, 141–64.

Beaudoin, G., Laurent, R., and Ohnenstetter, D. (1990) First report of platinum-group minerals at Blue Lake, Labrador Trough, Quebec. *Can. Mineral.*, **28**, 409–18.

Boudreau, A. E. (1988) Investigations of the Stillwater Complex IV. The role of volatiles in the petrogenesis of the J-M Reef, Minneapolis Adit section. Ibid., **26**, 193–208.

—— Mathez, E. A., and McCallum, I. S. (1986) Halogen geochemistry of the Stillwater and Bushveld Complexes: Evidence for Transport of the Platinum-Group Elements by Cl-Rich Fluids. *J. Petrol.*, **27**, 967–86.

Brynard, H. J., De Villiers, J. P. R., and Viljoen, E. A. (1976) A Mineral Investigation of the Merensky Reef of the Western Platinum Mine, near Marikana, South Africa. *Econ. Geol.*, **71**, 1299–1307.

Buchanan, D. L. (1988) *Platinum-Group Element Exploration.* Elsevier, Amsterdam, 21–35.

Cabri, L. J. and Laflamme, J. H. G. (1976) The mineralogy of the Platinum-Group Elements from some copper–nickel deposits of the Sudbury area, Ontario. *Econ. Geol.*, **71**, 1159–95.

—— —— (1981) Analyses of Minerals containing Platinum-Group Elements. In *Platinum-Group Elements: Mineralogy, Geology, Recovery* (L. J. Cabri, ed.). Can. Inst. of Min. & Met., Montreal, 151–74.

—— —— Stewart, J. M., Turner, K., and Skinner, B. J. (1978) On cooperite, braggite and vysotskite. *Am. Mineral.*, **63**, 832–9.

—— Rowland, J. F., Laflamme, J. H. G., and Stewart, J. M. (1979) Keithconnite, telluropalladinite and other Pd-Pt tellurides from the Stillwater Complex, Montana. *Can. Mineral.*, **17**, 589–94.

Campbell, I. H. and Barnes, S. J. (1984) A model for the geochemistry of the platinum-group elements in magmatic sulphide deposits. Ibid., **22**, 151–60.

Campbell, I. H. and Naldrett, A. J. (1979) The influence of silicate:sulphide ratios on the geochemistry of magmatic sulphides. *Econ. Geol.*, **74**, 1503–6.

——— and Barnes, S. J. (1983) A model for the origin of the platinum-rich sulphide horizons in the Bushveld and Stillwater Complexes. *J. Petrol.*, **24**, 133–85.

Cousins, C. A. and Vermakk, C. F. (1976) The contribution of South African ore deposits to the geochemistry of the Platinum-Group Metals. *Econ. Geol.*, **71**, 287–305.

Davis, G. and Tredoux, M. (1985) The platinum-group element and gold contents of the marginal rocks and sills of the Bushveld Complex. Ibid., **80**, 838–48.

Evans, D. M. and Buchanan, D. L. (1991) Application of petrographic studies to MSZ platinum-group element and base-metal mineralisation at Zinca prospect, Great Dyke, Zimbabwe. *Trans. Instn. Min. Metall. (Sect. B: Appl. earth sci.)*, **100**, B216–26.

Häkli, T. A., Hönninen, E., Vuorelainen, Y., and Papunen, H. (1976) Platinum-Group Minerals in the Hikura Nickel Deposit Finland. *Econ. Geol.*, **71**, 1206–13.

Harney, D. M. W. and Merkle, R. K. W. (1990) Pt–Pd minerals from the Upper Zone of the eastern Bushveld Complex, South Africa. *Can. Mineral.*, **28**, 619–628.

Haughton, D. R., Roeder, P. L. and Skinner, B. J. (1974) Solubility of sulphur in mafic magmas. *Econ. Geol.*, **69**, 451–7.

Haynes, L. (1983) The platinum mineralogy of the Great Dykes; some observations and new information. *Inst. Mining Research Annual Report,* Univ. Zimbabwe.

Helz, R. T. (1985) Interactions of sulphide-saturated basalts with PtFe and PdAgFe alloy capsules: experimental observations. *Can. Mineral.*, **23**, 326.

Johan, Z., Ohnenstetter, D., and Naldrett, A. J. (1989) Platinum-group minerals and associated oxides and base metal sulphides of the Main Sulphide Zone, Great Dyke, Zimbabwe. In *Abstracts—5th International Platinum Symposium* (H. Papunen, ed.), *Bull. Geol. Soc. Finland,* **No. 61,** Pt.1, 53–4.

Lightfoot, B. (1926) Platinum in Southern Rhodesia. *South. Rhod. Geol. Surv. Short Report,* **19**, 13 pp.

—— (1927) Traverses along the Great Dyke of Southern Rhodesia. *South. Rhod. Geol. Surv. Short Report,* **21**.

Lindsay, N. M. (1988) *The processing and recovery of the platinum-group elements.* Unpubl. Ph.D. Thesis, Univ. of the Witwatersrand, Johannesburg.

Macdonald, A. J. (1987) Ore Deposit Models #12. The Platinum-Group Element Deposits: classification and genesis. *Geoscience Canada,* **14**, 155–66.

Makovicky, E., Karup-Moller, S., Makovicky, M. and Rose-Hansen, J. (1990) Experimental Studies on the Phase Systems Fe–Ni–Pd–S and Fe–Pt–Pd–As–S Applied to PGE Deposits. *Mineral. Petrol.*, **42**, 307–19.

McCallum, M. E., Loucks, R. R., Carlson, R. R., Cooley, E. F. and Doerge, T. A. (1976) Platinum metals associated with hydrothermal copper ores of the New Rambler Mine, Medicine Bow Mountains, Wyoming. *Econ. Geol.*, **71**, 1429–50.

Naldrett, A. J. and Wilson, A. H. (1989) Distribution and controls of platinum group element mineralisation in Cyclic Unit 1 of the Great Dyke, Zimbabwe. In *Abstracts—5th International Platinum Symposium* (H. Papunen, ed.). *Bull. Geol. Soc. Finland,* **61**, Pt. 1, 3.

——— (1990) Horizontal and vertical variations in noble-metal distribution in the Great Dyke of Zimbabwe: A model for the origin of the PGE mineralisation by fractional segregation. *Chem. Geol.*, **88**, 279–300.

—— Brugmann, G. E., and Wilson, A. H. (1990) Models for the concentration of PGE in layered intrusions. *Can. Mineral.*, **28**, 389–408.

Peach, C. L., Mathez, E. A. and Keays, R. R. (1989) Sulfide melt-silicate melt distribution coefficients for the noble metals as deduced from MORBS. In *Abstracts—5th International Platinum Symposium* (H. Papunen, ed.). *Bull. Geol. Soc. Finland,* **61**, Pt. 1, 58.

Podmore, F. and Wilson, A. H. (1987) A reappraisal of the structure, geology and emplacement of the Great Dyke, Zimbabwe. In *Mafic Dyke Swarms* (H. C. Halls and W. F. Fahrig, eds.). *Geol. Assoc. Canada Sp. Paper,* **34**, 317–30.

Prendergast, M. D. (1990) Platinum-group minerals and hydrosilicate 'alteration' in Wedza–Mimosa Platinum Deposit, Great Dyke, Zimbabwe—genetic and metallurgical implications. *Trans. Instn. Min. Metall. (Sect. B: Appl. earth sci.)*, **99**, B91–105.

—— (1991) The Wedza-Mimosa platinum deposit, Great Dyke, Zimbabwe: layering and stratiform PGE mineralisation in a narrow mafic magma chamber. *Geol. Mag.*, **128**, 235–49.

—— and Keays, R. R. (1989) Controls of platinum-group element mineralisation and the origin of the PGE-rich Main Sulphide Zone in the Wedza Subchamber of the Great Dyke, Zimbabwe: implications for the genesis of, and exploration for, stratiform PGE mineralisation in layered intrusions. In *Magmatic Sulphides—The Zimbabwe Volume* (M. D. Prendergast and M. J. Jones, eds.). The Inst. of Min. & Met., London, 43–69.

—— and Wilson, A. H. (1989) The Great Dyke of Zimbabwe—II: Mineralisation and mineral deposits. In *Magmatic Sulphides—The Zimbabwe Volume* (M. D. Prendergast and M. J. Jones, eds.). The Inst. of Min. & Met., London, 21–42.

Raedeke, L. W. and Vian, R. W. (1986) A three-dimensional view of mineralisation in the Stillwater J-F Reef. *Econ. Geol.*, **81**, 1187–95.

Schweigart, H. (1967) Rhodesian Platinum. *Union Carbide Corporation progress report, September 15,* 4 pp.

—— and Fasso, F. J. (1967) Rhodesian Platinum. *Union Carbide Corporation progress report.* October 15, 15 pp.

Skinner, B. J., Luce, F. D., Dill, J. A., Ellis, D. E., Hagan, H. A. Lewis, D. M., Odell, D. A., Sverjensky, D. A. and Williams, N. (1976) Phase relations in ternary portions of the system Pt–Pd–Fe–As–S. *Econ. Geol.*, **71**, 1469–75.

Stumpfl, E. F. and Balhaus, C. G. (1986) Stratiform platinum deposits: New data and concepts. *Fortschr. Miner.*, **64**, 205–14.

Vermaak, C. F. (1976) The Merensky Reef—thoughts on its environment and genesis. *Econ. Geol.*, **71**, 1270–98.

—— and Hendriks, L. P. (1976) A review of the mineralogy of the Merensky Reef, with special reference to new data on the precious metal mineralogy. Ibid., **71**, 1244–69.

Wagner, P. A. (1929) *Platinum deposits and mines of South Africa.* C. Struik, (Pty) Ltd, Cape Town, 338 pp.

Wilson, A. H. (1982) The geology of the Great 'Dyke', Zimbabwe: the Ultramafic Rocks. *J. Petrol.*, **23**, 240–92.

—— (1992) The geology of the Great Dyke, Zimbabwe: crystallisation, layering and cumulate formation in the P1 Pyroxenite of Cyclic Unit 1 of the Darwendale Subchamber. Ibid., **33**, 611–63.

—— and Prendergast, M. D. (1989) The Great Dyke of Zimbabwe: I: Tectonic setting, stratigraphy, petrology, structure, emplacement and crystallisation. In *Magmatic Sulphides—The Zimbabwe Volume* (M. D. Prendergast and M. J. Jones, eds.). The Inst. of Min. & Met., London, 1–20.

—— and Tredoux, M. (1990) Lateral and vertical distribution of the platinum group elements, and petrogenetic controls on the sulphide mineralisation, in the P1 Pyroxenite layer of the Darwendale Subchamber of the Great Dyke, Zimbabwe. *Econ. Geol.*, **85**, 556–84.

—— Naldrett, A. J., and Tredoux, M. (1989) Distribution and controls of platinum-group element and base metal mineralisation in the Darwendale Subchamber of the Great Dyke, Zimbabwe. *Geology*, **17**, 649–52.

Zealley, A. E. V. (1918) The occurrence of platinum in Southern Rhodesia. *South Rhod. Geol. Surv. Short Report*, **3**.

Zientek, M. L., Fries, T. L. and Vian, R. W. (1990) As, Bi, Hg, S, Sb, Sn and Te geochemistry of the J–M Reef, Stillwater Complex, Montana: constraints on the origin of PGE-enriched sulphides in layered intrusions. In *Geochemistry of Platinum-Group Elements*, (C. E. Dunn, G. C. Curtin, and G. E. M. Hall, eds.). *J. Geochem. Explor.*, **37**, 51–73.

[*Manuscript received 26 February 1992: revised 16 December 1992*]